

Production of doubly charged scalars from the decay of a heavy SM-like Higgs boson in the Higgs Triplet Model

A.G. Akeroyd* and S. Moretti†

¹*School of Physics and Astronomy, University of Southampton,
Highfield, Southampton SO17 1BJ, United Kingdom, and*

²*Particle Physics Department, Rutherford Appleton Laboratory,
Chilton, Didcot, Oxon OX11 0QX, United Kingdom*

Abstract

The Higgs Triplet Model (HTM) of neutrino mass generation predicts the existence of doubly charged Higgs bosons ($H^{\pm\pm}$). In the HTM a scalar eigenstate (H_2) is dominantly composed of the scalar field from the isospin doublet, and could be significantly heavier than $H^{\pm\pm}$. Such a scenario would allow the possibility of a large branching ratio for the decay $H_2 \rightarrow H^{++}H^{--}$. From the production mechanism of gluon-gluon fusion, $gg \rightarrow H_2$, the above decay mode would give rise to pair production of doubly charged Higgs bosons ($H^{++}H^{--}$) with a cross section which could be significantly larger than the cross sections for the standard production mechanisms $q\bar{q} \rightarrow \gamma, Z \rightarrow H^{++}H^{--}$ and $q'\bar{q} \rightarrow W \rightarrow H^{\pm\pm}H^\mp$. We discuss the phenomenological consequences for the ongoing searches for $H^{\pm\pm}$ at the Tevatron and at the LHC.

PACS numbers: 14.80.Fd, 12.60.Fr

*Electronic address: a.g.akeroyd@soton.ac.uk

†Electronic address: S.Moretti@soton.ac.uk

I. INTRODUCTION

The established evidence that neutrinos oscillate and possess a small mass below the electron volt (eV) scale [1] necessitates physics beyond the Standard Model (SM), which could manifest itself at the CERN Large Hadron Collider (LHC) and the Fermilab Tevatron, and/or in low energy experiments which search for lepton flavour violation (LFV) [2]. Consequently, models of neutrino mass generation which can be probed at present and forthcoming experiments are of great phenomenological interest.

Neutrinos may obtain mass via the vacuum expectation value (vev) of a neutral Higgs boson in an isospin triplet representation [3–7]. A particularly simple implementation of this mechanism of neutrino mass generation is the “Higgs Triplet Model” (HTM) in which the SM Lagrangian is augmented solely by a $SU(2)$ triplet of scalar particles Δ with hypercharge $Y = 2$ [3, 6, 7]. In the HTM, neutrinos acquire a Majorana mass given by the product of a triplet Yukawa coupling (h_{ij} , with $i, j = e, \mu, \tau$) and a triplet vev (v_Δ). Consequently, there is a direct connection between h_{ij} and the neutrino mass matrix, which gives rise to phenomenological predictions for processes which depend on h_{ij} . A distinctive signal of the HTM would be the observation of doubly charged Higgs bosons ($H^{\pm\pm}$) whose mass ($M_{H^{\pm\pm}}$) may be of the order of the electroweak scale. Such particles could be produced with sizeable rates at hadron colliders via the processes $q\bar{q} \rightarrow H^{++}H^{--}$ [8–12] and $q'\bar{q} \rightarrow H^{\pm\pm}H^\mp$ [8, 13, 14]. The first searches for $H^{\pm\pm}$ at a hadron collider were carried out at the Fermilab Tevatron, assuming the production channel $q\bar{q} \rightarrow H^{++}H^{--}$ and decay $H^{\pm\pm} \rightarrow \ell_i^\pm \ell_j^\pm$. The mass limits $M_{H^{\pm\pm}} > 110 \rightarrow 150$ GeV [15–18] were derived, with the strongest limits being for $\ell = e, \mu$ [15–17]. The branching ratios (BRs) for $H^{\pm\pm} \rightarrow \ell_i^\pm \ell_j^\pm$ depend on h_{ij} and are predicted in the HTM in terms of the parameters of the neutrino mass matrix [14, 19, 20]. Detailed quantitative studies of $\text{BR}(H^{\pm\pm} \rightarrow \ell_i^\pm \ell_j^\pm)$ (and $\text{BR}(H^\pm \rightarrow \ell_i^\pm \nu)$) in the HTM have been performed in [21–26] with particular emphasis given to their sensitivity to the Majorana phases and the absolute neutrino mass i.e. parameters which cannot be probed in neutrino oscillation experiments. Simulations of the detection prospects of $H^{\pm\pm}$ at the LHC with $\sqrt{s} = 14$ TeV previously focussed on $q\bar{q} \rightarrow \gamma^*, Z^* \rightarrow H^{++}H^{--}$ only [27, 28], but recent studies now include the mechanism $q'\bar{q} \rightarrow H^{\pm\pm}H^\mp$ [24, 25, 29]. The first search for $H^{\pm\pm}$ at the LHC with $\sqrt{s} = 7$ TeV [30] has recently been performed for both production mechanisms $q\bar{q} \rightarrow H^{++}H^{--}$ and $q\bar{q}' \rightarrow H^{\pm\pm}H^\mp$, for the decay channels $H^{\pm\pm} \rightarrow \ell_i^\pm \ell_j^\pm$ and $H^\pm \rightarrow \ell_i^\pm \nu$ (where $i, j = e, \mu, \tau$).

In the HTM there are two electrically neutral mass eigenstates which are CP-even scalars. These are denoted by H_1 and H_2 , with $M_{H_1} < M_{H_2}$. One of the eigenstates is dominantly composed of the isospin doublet field (and plays the role of the SM Higgs boson) while the other eigenstate is dominantly composed of the real part of the neutral triplet field. The mixing angle is small because it depends on the small ratio $v_\Delta/v < 0.03$ (where $v = 246$ GeV, the vev of the doublet field). In phenomenological studies of the HTM it is usually assumed that the lighter eigenstate H_1 is the one which is dominantly composed of the isospin doublet field. Therefore the phenomenology of H_1 is more or less identical to that of the SM-Higgs boson. The converse case of the heavier eigenstate H_2 being the one which is dominantly composed of the isospin doublet field is possible in the HTM, and has been mentioned in [31–33]. However, no detailed study of the phenomenology of H_2 in such a scenario has been carried out. Importantly, if $M_{H_2} > 2M_\phi$ [33] (where ϕ is one of the dominantly triplet eigenstates $H_1, A^0, H^\pm, H^{\pm\pm}$) then new decay channels for H_2 would be possible. This would give rise to a phenomenology of H_2 which differs somewhat from that of the SM

Higgs boson. In this work we focus on the case of $M_{H_2} > 2M_{H^{\pm\pm}}$, because a new production mechanism for $H^{\pm\pm}$ would be possible, namely gluon-gluon fusion $gg \rightarrow H_2$ followed by decay $H_2 \rightarrow H^{++}H^{--}$. The case of $M_{H_2} > 2M_{H^{\pm\pm}}$ necessarily requires $M_{H_2} \gtrsim 200$ GeV, a mass region which is now being probed for the first time by the LHC for the decay channels to SM particles, $H_2 \rightarrow WW$ and $H_2 \rightarrow ZZ$ [34, 35].

Our work is organised as follows. In section II we describe the theoretical structure of the HTM. In section III the parameter space for $M_{H_2} > 2M_\phi$ (where ϕ is one of $H_1, A^0, H^\pm, H^{\pm\pm}$) is described. In section IV the formulae for the decay widths of $H_2 \rightarrow H^{++}H^{--}, H^+H^-, A^0A^0, H_1H_1$ are presented. Section V contains a numerical analysis of the magnitude of the branching ratios of the above channels, as well as a quantitative study of the cross section for pair production of $H^{\pm\pm}$ via $gg \rightarrow H_2$, with decay $H_2 \rightarrow H^{++}H^{--}$. Conclusions are given in section VI.

II. THE HIGGS TRIPLET MODEL

In the HTM [3, 6, 7] a $I = 1, Y = 2$ complex $SU(2)_L$ isospin triplet of scalar fields is added to the SM Lagrangian. Such a model can provide a Majorana mass for the observed neutrinos without the introduction of a right-handed neutrino via the gauge invariant Yukawa interaction:

$$\mathcal{L} = h_{ij}\psi_{iL}^T C i\tau_2 \Delta \psi_{jL} + h.c \quad (1)$$

Here $h_{ij}(i, j = e, \mu, \tau)$ is a complex and symmetric coupling, C is the Dirac charge conjugation operator, τ_2 is a Pauli matrix, $\psi_{iL} = (\nu_i, \ell_i)_L^T$ is a left-handed lepton doublet, and Δ is a 2×2 representation of the $Y = 2$ complex triplet fields:

$$\Delta = \begin{pmatrix} \delta^+/\sqrt{2} & \delta^{++} \\ \delta^0 & -\delta^+/\sqrt{2} \end{pmatrix} \quad (2)$$

A non-zero triplet vacuum expectation value $\langle \Delta^0 \rangle$ gives rise to the following mass matrix for neutrinos:

$$m_{ij} = 2h_{ij}\langle \Delta^0 \rangle = \sqrt{2}h_{ij}v_\Delta \quad (3)$$

The necessary non-zero v_Δ arises from the minimisation of the most general $SU(2) \otimes U(1)_Y$ invariant Higgs potential, which is written as follows [19, 20] (with $\Phi = (\phi^+, \phi^0)^T$):

$$\begin{aligned} V(H, \Delta) = & -m_H^2 H^\dagger H + \lambda(H^\dagger H)^2 + M_\Delta^2 \text{Tr} \Delta^\dagger \Delta + (\mu H^T i\sigma_2 \Delta^\dagger H + \text{h.c.}) \\ & + \lambda_1 (H^\dagger H) \text{Tr} \Delta^\dagger \Delta + \lambda_2 (\text{Tr} \Delta^\dagger \Delta)^2 + \lambda_3 \text{Tr} (\Delta^\dagger \Delta)^2 + \lambda_4 H^\dagger \Delta \Delta^\dagger H \end{aligned} \quad (4)$$

Here $m_H^2 < 0$ in order to ensure $\langle \phi^0 \rangle = v/\sqrt{2}$ which spontaneously breaks $SU(2) \otimes U(1)_Y$ to $U(1)_Q$, and $M_\Delta^2 (> 0)$ is the mass term for the triplet scalars. In the model of Gelmini-Roncadelli [36] the term $\mu(\Phi^T i\tau_2 \Delta^\dagger \Phi)$ is absent, which leads to spontaneous violation of lepton number for $M_\Delta^2 < 0$. The resulting Higgs spectrum contains a massless triplet scalar (a Majoron, J) and another light scalar (H^0). Pair production via $e^+e^- \rightarrow H^0 J$ would give a large contribution to the invisible width of the Z boson and this model was excluded at the CERN Large Electron Positron Collider (LEP). The inclusion of the term $\mu(\Phi^T i\tau_2 \Delta^\dagger \Phi)$ explicitly breaks lepton number when Δ is assigned $L = 2$, and eliminates

the Majoron [3, 6, 7]. Thus the scalar potential in eq. (4) together with the triplet Yukawa interaction of eq. (1) lead to a phenomenologically viable model of neutrino mass generation. For small v_Δ/v , the expression for v_Δ resulting from the minimisation of V is:

$$v_\Delta \simeq \frac{\mu v^2}{\sqrt{2}(M_\Delta^2 + v^2(\lambda_1 + \lambda_4)/2)} \quad (5)$$

For large M_Δ compared to v one has $v_\Delta \simeq \mu v^2/\sqrt{2}M_\Delta^2$, which is sometimes referred to as the “Type II seesaw mechanism” and would naturally lead to a small v_Δ . Recently there has been much interest in the scenario of light triplet scalars ($M \approx v$), (especially the distinctive doubly charged scalar, $H^{\pm\pm}$), within the discovery reach of the LHC, for which eq. (5) leads to $v_\Delta \approx \mu$. In extensions of the HTM the term $\mu(\Phi^T i\tau_2 \Delta^\dagger \Phi)$ may arise in various ways: i) it can be generated at tree level via the vev of a Higgs singlet field [37]; ii) it can arise at higher orders in perturbation theory [20]; iii) it can originate in the context of extra dimensions [19]; iv) it can arise in models with an additional heavy scalar triplet [38].

Some phenomenological studies focus on a simplified scalar potential (e.g. Ref. [24]) in which the quartic couplings λ_i (where $i = 1, 2, 3, 4$) involving the triplet field Δ are neglected. The resulting scalar potential then depends on four parameters ($-m_H^2$, λ , μ , M_Δ), but only three parameters are independent because the VEV for the doublet field ($v = 246$ GeV) is fixed by the mass of W^\pm . The three independent parameters are usually chosen as $\lambda, v_\Delta, M_\Delta$ or λ, v_Δ, μ (see eq. (5)). The inclusion of λ_i generates additional trilinear and quartic couplings among the scalar mass eigenstates. The terms with λ_1 and λ_4 , which involve both triplet and doublet fields, are of particular interest because they can give a sizeable contribution to the masses of the scalar eigenstates (see below). A detailed study of the theoretical constraints on the scalar potential (e.g. vacuum stability, unitarity and perturbativity) has been carried out in [33].

An upper limit on v_Δ can be obtained from considering its effect on the parameter $\rho (= M_W^2/M_Z^2 \cos^2 \theta_W)$. In the SM $\rho = 1$ at tree-level, while in the HTM one has (where $x = v_\Delta/v$):

$$\rho \equiv 1 + \delta\rho = \frac{1 + 2x^2}{1 + 4x^2} \quad (6)$$

The measurement $\rho \approx 1$ leads to the bound $v_\Delta/v \lesssim 0.03$, or $v_\Delta \lesssim 8$ GeV. Production mechanisms which depend on v_Δ (i.e. $pp \rightarrow W^{\pm*} \rightarrow W^\mp H^{\pm\pm}$ and fusion via $W^{\pm*}W^{\pm*} \rightarrow H^{\pm\pm}$ [12, 39]) are not competitive with the processes $q\bar{q} \rightarrow H^{++}H^{--}$ and $\bar{q}q' \rightarrow H^{\pm\pm}H^\mp$ at the energies of the Fermilab Tevatron, but such mechanisms could be the dominant source of $H^{\pm\pm}$ at the LHC if $v_\Delta = \mathcal{O}(1 \text{ GeV})$ and $M_{H^{\pm\pm}} > 500$ GeV. At the 1-loop level, v_Δ must be renormalised and explicit analyses lead to bounds on its magnitude similar to the above bound from the tree-level analysis, e.g. see [40, 41].

The scalar eigenstates in the HTM are as follows: i) the charged scalars $H^{\pm\pm}$ and H^\pm ; ii) the CP-even neutral scalars H_1 and H_2 ; iii) a CP-odd neutral scalar A^0 . The doubly charged $H^{\pm\pm}$ is entirely composed of the triplet scalar field $\Delta^{\pm\pm}$, while the remaining eigenstates are in general mixtures of the doublet and triplet fields. However, such mixing is proportional to the triplet vev, and hence small *even if* v_Δ assumes its largest value of a few GeV.¹

¹ A large mixing angle is possible in the CP-even sector provided that $M_{H_1} \sim M_{H_2}$ [31–33].

III. SCENARIO OF A HEAVY SM-LIKE HIGGS BOSON (H_2) IN THE HTM

In the HTM there are two CP-even mass eigenstates, which we denote by H_1 and H_2 (where both $M_{H_2} > M_{H_1}$ and $M_{H_1} > M_{H_2}$ are possible). Their compositions in terms of the original fields of the Lagrangian are as follows:

$$H_2 = \cos \theta_0 h^0 + \sin \theta_0 \Delta^0 \quad H_1 = -\sin \theta_0 h^0 + \cos \theta_0 \Delta^0 \quad (7)$$

Here h^0 is the real part of the electrically neutral doublet field ϕ^0 , and Δ^0 is the real part of the electrically neutral triplet field δ^0 . The mixing angle θ_0 is very small,² being of order 0.03 at most ($\sin \theta_0 \sim v_\Delta/v$). Hence H_2 is essentially composed of the doublet field h^0 , with couplings to the fermions and gauge bosons which are almost identical to those of the SM Higgs boson, while H_1 is mainly composed of the triplet field Δ^0 .

The explicit expression for the 2×2 CP-even scalar mass matrix for the scalar potential in eq. (4) is given in several works e.g. [31–33]. Neglecting the small off-diagonal elements in this mass matrix, the approximate expressions for the squared masses of H_1 and H_2 are as follows:

$$M_{H_2}^2 = 2\lambda v^2 \quad (8)$$

$$M_{H_1}^2 = M_\Delta^2 + \left(\frac{\lambda_1}{2} + \frac{\lambda_4}{2}\right)v^2 + 3(\lambda_2 + \lambda_3)v_\Delta^2 \quad (9)$$

The squared mass of the (dominantly triplet) CP-odd A^0 is given by:

$$M_{A^0}^2 = M_\Delta^2 + \left(\frac{\lambda_1}{2} + \frac{\lambda_4}{2}\right)v^2 + (\lambda_2 + \lambda_3)v_\Delta^2 \quad (10)$$

The squared mass of the (dominantly triplet) H^\pm is given by:

$$M_{H^\pm}^2 = M_\Delta^2 + \left(\frac{\lambda_1}{2} + \frac{\lambda_4}{4}\right)v^2 + (\lambda_2 + \sqrt{2}\lambda_3)v_\Delta^2 \quad (11)$$

Finally, the squared mass of the (purely triplet) doubly-charged scalar ($H^{\pm\pm} = \delta^{\pm\pm}$) is given by:

$$M_{H^{\pm\pm}}^2 = M_\Delta^2 + \frac{\lambda_1}{2}v^2 + \lambda_2 v_\Delta^2 \quad (12)$$

One can see that the squared mass of the (dominantly doublet) H_2 is simply given by $2\lambda v^2$, as in the SM. In the expressions for the masses of $M_{A^0}^2$, $M_{H_1}^2$, $M_{H^\pm}^2$ and $M_{H^{\pm\pm}}^2$ there is a common term $M_\Delta^2 + \frac{\lambda_1}{2}v^2$. It is evident that the mass scales for H_2 and the dominantly triplet scalars ($A^0, H_1, H^\pm, H^{\pm\pm}$) are unrelated, the former being set by $2\lambda v^2$ and the latter by $M_\Delta^2 + \frac{\lambda_1}{2}v^2$. Neglecting the terms which are proportional to the small parameter v_Δ , one can see that there are only two possible mass hierarchies for the triplet scalars, with the magnitude of the mass splitting being controlled by λ_4 (and $M_{A^0} = M_{H_1}$):

$$M_{A^0}, M_{H_1} < M_{H^\pm} < M_{H^{\pm\pm}} \quad \text{for } \lambda_4 < 0 \quad (13)$$

$$M_{H^{\pm\pm}} < M_{H^\pm} < M_{A^0}, M_{H_1} \quad \text{for } \lambda_4 > 0 \quad (14)$$

² The mixing angle can be maximal in the region of degeneracy $M_{H_2} \sim M_{H_1}$, but it quickly becomes small ($\sim v_\Delta/v$) with increasing mass splitting $|M_{H_2} - M_{H_1}|$ [31–33].

In studies of the HTM it is sometimes assumed that $M_\Delta^2 \gg 2\lambda v^2$ i.e. $M_{H^{\pm\pm}}, M_{H^\pm}, M_{H_1}, M_{A^0} \gg M_{H_2}$. The motivation for this scenario is to have a “seesaw type” explanation for the smallness of v_Δ in eq. (5). However, for M_Δ much larger than the TeV scale there would be no hope of observing the triplet scalars at the LHC. In recent years there has been much interest in the study of the HTM as a TeV scale model of neutrino mass generation [10–14, 19–29] i.e. not invoking a large mass scale for M_Δ . In these studies it is assumed (either explicitly or implicitly) that $M_\Delta^2 > 2\lambda v^2$, with $M_\Delta < 1$ TeV.

The converse case where $M_\Delta^2 + \frac{\lambda_1}{2}v^2 < 2\lambda v^2$ is rarely considered. In [31–33] the possibility of $M_{H_2} > M_{H^{\pm\pm}}, M_{H^\pm}, M_{H_1}, M_{A^0}$ has been mentioned, and in [33] the case of $M_{H_2} > 2M_\phi$ (where ϕ is one of $H^{\pm\pm}, H^\pm, H_1, A^0$) is explicitly discussed. However, in these works there is no study of the phenomenology of H_2 at hadron colliders for the case of $M_{H_2} > 2M_\phi$, and how its experimental signature might differ from that of the SM Higgs Boson. Importantly, if $M_{H_2} > 2M_\phi$ then new decay channels for H_2 become possible,³ namely $H_2 \rightarrow H^{++}H^{--}, H^+H^-, H_1H_1, A^0A^0$.

In this case the phenomenology of H_2 in the HTM could be different to that of the SM Higgs boson, because the new decay channels (if open kinematically) would compete with the usual decays of H_2 to SM particles (i.e. $H_2 \rightarrow WW, ZZ, t\bar{t}$). Of particular interest is the decay $H_2 \rightarrow H^{++}H^{--}$, for which the condition $M_{H_2} > 2M_{H^{\pm\pm}}$ is necessary. If its branching ratio were sizeable then the production of H_2 via gluon-gluon fusion $gg \rightarrow H_2$ followed by the decay $H_2 \rightarrow H^{++}H^{--}$ would be an additional way to produce a pair of $H^{\pm\pm}$ at hadron colliders.

We note that the condition $M_{H_2} > 2M_{H^{\pm\pm}}$ necessarily requires $M_{H_2} \gtrsim 200$ GeV in order to respect the current lower bounds on $M_{H^{\pm\pm}}$ from direct searches. At first sight, such a heavy SM-like H_2 would appear to be in conflict with experimental data, since it is well known that the Higgs boson in the SM is expected to be lighter than 200 GeV in order not to give an unacceptably large contribution to electroweak precision observables. In the context of the SM the case of $M_{H_2} \gtrsim 200$ GeV is quite strongly disfavoured, although this fact has not dissuaded direct searches in this mass region at the LHC [34, 35]. However, the bound $M_{H_2} \gtrsim 200$ GeV cannot strictly be applied to the HTM, due to the additional scalar particles and the different renormalisation procedure, the latter being necessary because of the presence of the triplet vev (v_Δ). Dedicated analyses in models with scalar triplets have shown that a heavy (up to 1 TeV) SM-like Higgs boson can be made consistent with electroweak precision measurements [40, 41]. These studies are for a model with a real $Y = 0$ scalar triplet, which has no doubly charged scalar and gives $\rho > 1$ at tree level, in contrast to the HTM which has $\rho < 1$ at tree level, (eq. (6)). One can see in [41] that the condition $M_{H_2} > 2M_\phi$ (where ϕ is one of the $Y = 0$ triplet scalars) can be accommodated. Although there is no explicit study in the HTM, we expect this result to also hold due to its greater number of free parameters (i.e. particle masses). In our numerical analysis we will treat $M_{H_2} < 700$ GeV and $M_{H_2} > 2M_{H^{\pm\pm}}$ as permissible parameter space in the HTM.

From a phenomenological point of view, a heavy ($\gg 200$ GeV) SM-like Higgs boson is attractive because it would be discovered more quickly at the LHC than a light SM-like Higgs boson with mass < 140 GeV. The region of $200 \text{ GeV} < M_{H_2} < 500 \text{ GeV}$, for which the decays $H_2 \rightarrow ZZ$ and $H_2 \rightarrow WW$ are dominant in the SM, is a mass range where the LHC has sensitivity to cross sections which are much smaller than that of the SM Higgs boson. The

³ The scenario of a heavy SM-like Higgs boson decaying to singly charged scalars, $h^0 \rightarrow H^+H^-$, has been discussed in the Two Higgs Doublet Model [42].

first searches at the LHC for a SM Higgs with $M_{H_2} > 200$ GeV have already been carried out. The ATLAS collaboration (with 36 pb^{-1} of integrated luminosity) has searched for $H_2 \rightarrow ZZ$ with the decay modes $ZZ \rightarrow \ell^+ \ell^- \nu \nu$, $ZZ \rightarrow \ell^+ \ell^- q \bar{q}$ and $ZZ \rightarrow \ell^+ \ell^- \ell^+ \ell^-$, as well as $H_2 \rightarrow WW$ with the decay mode $WW \rightarrow \ell \nu q' \bar{q}$ [34]. The CMS collaboration has searched for $H_2 \rightarrow WW$ with the decay mode $WW \rightarrow \ell \nu \ell \nu$ [35]. Production of H_2 is assumed to be via gluon-gluon fusion, $gg \rightarrow H_2$, and cross sections which are an order of magnitude above the prediction of the SM are currently being excluded at 95% c.l. By the end of the $\sqrt{s} = 7$ TeV run (in which a few fb^{-1} of integrated luminosity will be accumulated), the sensitivity in these channels will be sufficient to exclude or provide evidence for the SM Higgs boson at a high confidence level in the region $200 \text{ GeV} < M_{H_2} < 500 \text{ GeV}$. If the branching ratios of $H_2 \rightarrow H^{++}H^{--}$, H^+H^- , H_1H_1 , A^0A^0 were sizeable then discovery of H_2 in the channels $H_2 \rightarrow ZZ$ and $H_2 \rightarrow WW$ would require more integrated luminosity.

IV. THE DECAYS $H_2 \rightarrow \phi\phi$ WITH $\phi = H^{\pm\pm}, H^\pm, H_1, A^0$

There are four decay channels of H_2 to pairs of scalars in the HTM: $H_2 \rightarrow H^{++}H^{--}$, $H_2 \rightarrow H^+H^-$, $H_2 \rightarrow A^0A^0$ and $H_2 \rightarrow H_1H_1$. If $M_{H_2} > 2M_\phi$ (where $\phi = H^{\pm\pm}, H^\pm, H_1, A^0$) one can treat this as a two-body decay to a pair of on-shell ϕ . If $M_{H_2} < 2M_\phi$ we consider the partial width to be zero. Between one and four of the decays $H_2 \rightarrow \phi\phi$ can be open kinematically, depending on the mass splitting among ϕ (which is controlled by λ_4 in eq. (13) and eq. (14). For $\lambda_4 > 0$ the lightest of the triplet scalars is $H^{\pm\pm}$. In this scenario, once values of M_{H_2} and $M_{H^{\pm\pm}}$ are chosen such that $M_{H_2} > 2M_{H^{\pm\pm}}$ there will be a value of λ_4 above which only $H_2 \rightarrow H^{++}H^{--}$ is kinematically open. This will be the scenario where $\text{BR}(H_2 \rightarrow H^{++}H^{--})$ is maximal.

The Feynman rules for the scalar trilinear couplings which mediate the decays are as follows (omitting a factor of $-i$):

$$C_{H_2H^{++}H^{--}} = \lambda_1 v \quad (15)$$

$$C_{H_2H^+H^-} = (\lambda_1 + \frac{\lambda_4}{2})v \quad (16)$$

$$C_{H_2H_1H_1}, C_{H_2A^0A^0} = (\lambda_1 + \lambda_4)v \quad (17)$$

Here we consider H_2 to be entirely composed of the isospin doublet scalar field, which is true to a very good approximation. One can see that $C_{H_2H^{++}H^{--}}$ is controlled only by λ_1 , while the other trilinear couplings depend on both λ_1 and λ_4 . If λ_1 and λ_4 are sizeable, then the branching ratios for $H_2 \rightarrow H^{++}H^{--}$, $H_2 \rightarrow H^+H^-$, $H_2 \rightarrow H_1H_1$, and $H_2 \rightarrow A^0A^0$ could be non-negligible.

One can use a generic formula for the decay rate for the four channels:

$$\Gamma(H_2 \rightarrow \phi\phi) = \delta_H \frac{|C_{H_2\phi\phi}|^2}{32\pi M_{H_2}} \left(1 - \frac{4M_\phi^2}{M_{H_2}^2}\right)^{1/2} \quad (18)$$

Here $\delta_H = 2$ for $\phi = H^{\pm\pm}, H^\pm$ (i.e. non-identical particles in the final state) and $\delta = 1$ for $\phi = H_1, A^0$ (i.e. identical particles in the final state)

It is clear that the two crucial parameters for a large $\text{BR}(H_2 \rightarrow H^{++}H^{--})$ are λ_1 (which determines the strength of the coupling $|C_{H_2H^{++}H^{--}}|$ in eq. (15) and $M_{H^{\pm\pm}}$ (which determines the suppression from phase space). In our numerical analysis we shall take

$M_{H^{\pm\pm}}$ as an input parameter. As can be seen from eq. (12), the dominant contribution to $M_{H^{\pm\pm}}^2$ is from the two terms $M_\Delta^2 + \lambda_1 v^2/2$. Therefore, by taking λ_1 and $M_{H^{\pm\pm}}$ as input parameters the value of M_Δ^2 is determined. We will be focussing on the parameter space of $90 \text{ GeV} < M_{H^{\pm\pm}} < 300 \text{ GeV}$ and $0 < \lambda_1 < 4$, and consequently $M_\Delta^2 < 0$ when $M_{H^{\pm\pm}}^2 < \lambda_1 v^2/2$. In the scenario of $M_\Delta^2 < 0$ the positive mass of $M_{H^{\pm\pm}}$ is obtained from the term $\lambda_1 v^2/2$. Alternatively, one could consider $\lambda_1 < 0$ and $M_\Delta^2 > 0$. The crucial point here is that the parameters M_Δ^2 and λ_1 should have opposite signs if one wishes to have large $|\lambda_1|$ (in order to enhance $|C_{H_2 H^{++} H^{--}}|$) together with a fairly light $H^{\pm\pm}$.

We now summarise the current lower limits on $M_{H^{\pm\pm}}$ from direct searches. There have been searches for the decay channels $H^{\pm\pm} \rightarrow \ell_i^\pm \ell_j^\pm$ for $i, j = e, \mu, \tau$ (these are the dominant decay channels for $v_\Delta \lesssim 0.1 \text{ MeV}$) at LEP [43], Tevatron [15–18] and the LHC [30] (CMS Collaboration). The strongest mass limits for the decays $H^{\pm\pm} \rightarrow ee, e\mu, \mu\mu$ are from the LHC search, which obtained $M_{H^{\pm\pm}} > 144, 154, 156 \text{ GeV}$ respectively, assuming $\text{BR} = 100\%$ in a given channel. Separate searches for three and four leptons (which have significantly different backgrounds) were performed. These limits are weakened considerably for the case of $\text{BR} < 100\%$ because the event number for the signal is proportional to the square of the branching ratio (BR^2). In [30] both production mechanisms $q\bar{q} \rightarrow \gamma^*, Z^* \rightarrow H^{++} H^{--}$ and $q'\bar{q} \rightarrow W \rightarrow H^{\pm\pm} H^\mp$ were considered (with the assumption $M_{H^{\pm\pm}} = M_{H^\pm}$), which increases the sensitivity in the three-lepton channel. For the decays involving one τ , namely $H^{\pm\pm} \rightarrow e\tau, \mu\tau$, the limit $M_{H^{\pm\pm}} > 106 \text{ GeV}$ was derived in both channels at the LHC [30], with stronger limits from the Tevatron ($M_{H^{\pm\pm}} > 112 \text{ GeV}$ and 114 GeV respectively) obtained in [18]. The only search for $H^{\pm\pm} \rightarrow \tau^\pm \tau^\pm$ at a hadron collider is the LHC search in [30], which derived the limit $M_{H^{\pm\pm}} \gtrsim 80 \text{ GeV}$.

We will take $M_{H^{\pm\pm}} = 90 \text{ GeV}$ as our lowest value for the mass of $H^{\pm\pm}$, and this is allowed for certain choices of branching ratios of $H^{\pm\pm}$. As explained above, the limits on $M_{H^{\pm\pm}}$ from hadron colliders are weakest for those channels which involve τ . In contrast, the limit from the LEP searches of $M_{H^{\pm\pm}} \gtrsim 100 \text{ GeV}$ applies to all the decays $H^{\pm\pm} \rightarrow \ell_i^\pm \ell_j^\pm$ with $i, j = e, \mu, \tau$. The search strategy at LEP requires four leptons and so the event number for the signal is proportional to BR^2 . The scenario of $M_{H^{\pm\pm}} = 90 \text{ GeV}$ is compatible with the all the above searches provided that the decays involving τ are dominant e.g. choices like $\text{BR}(H^{\pm\pm} \rightarrow e\tau, \mu\tau, \tau\tau)$ of around 33%. It is not necessary to have $\text{BR}(H^{\pm\pm} \rightarrow ee, e\mu, \mu\mu)$ totally absent for $M_{H^{\pm\pm}} = 90 \text{ GeV}$, and BRs of the order of 10% for these channels can be accommodated because the event number is proportional to BR^2 , and for $\text{BR} = 10\%$ this is a large suppression factor. We note that the sum of $\text{BR}(H^{\pm\pm} \rightarrow ee, e\mu, \mu\mu)$ cannot be taken arbitrarily small in the HTM because the Yukawa couplings h_{ij} are related to the neutrino mass matrix via eq. (3). The allowed values of $\text{BR}(H^{\pm\pm} \rightarrow \ell_i^\pm \ell_j^\pm)$ in the HTM have been studied in detail in [21–26], and in [25] it can be seen explicitly that the sum of $\text{BR}(H^{\pm\pm} \rightarrow ee, e\mu, \mu\mu)$ must be greater than around 5%.

Very recently the searches for $H^{\pm\pm} \rightarrow ee, e\mu, \mu\mu$ by the CDF collaboration in [15] (which used 0.24 fb^{-1}) were updated using 6.1 fb^{-1} [44]. Mass limits of $M_{H^{\pm\pm}} > 225, 210, 245 \text{ GeV}$ were obtained, again assuming $\text{BR} = 100\%$. In these searches the event number for the signal is linear in BR , and for $\text{BR} \sim 3\%(15\%)$ the limit $M_{H^{\pm\pm}} > 245 \text{ GeV}$ for $H^{\pm\pm} \rightarrow \mu\mu$ would weaken to $M_{H^{\pm\pm}} > 100 \text{ GeV}$ (150 GeV). Note that these mass limits in [44] only assume production of $H^{\pm\pm}$ from $q\bar{q} \rightarrow \gamma^*, Z^* \rightarrow H^{++} H^{--}$. The inclusion of $q'\bar{q} \rightarrow W \rightarrow H^{\pm\pm} H^\mp$ would allow larger values of $M_{H^{\pm\pm}}$ to be probed. Finally, if the decay $H^{\pm\pm} \rightarrow W^\pm W^\pm$ is dominant (which is the case for $v_\Delta \gtrsim 0.1 \text{ MeV}$) then $M_{H^{\pm\pm}} = 90 \text{ GeV}$ is permitted because there have been no direct searches for this channel in the context of models with $H^{\pm\pm}$. We

will respect the all the above mass limits in our numerical analysis, the most stringent ones being for the channels $H^{\pm\pm} \rightarrow e^\pm e^\pm, e^\pm \mu^\pm$ and $\mu^\pm \mu^\pm$.

We will only consider the scenario of $M_{H_2} > 200$ GeV for which the decay channels $H_2 \rightarrow WW$ and $H_2 \rightarrow ZZ$ can be treated as two-body decays. The expressions for their partial decay widths are as follows:

$$\Gamma(H_2 \rightarrow WW) = \frac{\sqrt{2}G_F M_{H_2}^3}{32\pi} (1 - 4\kappa_W + 12\kappa_W^2)(1 - 4\kappa_W)^{1/2} \delta_W \quad (19)$$

with $\kappa_W = M_W^2/M_{H_2}^2$ and $\delta_W = 2$.

$$\Gamma(H_2 \rightarrow ZZ) = \frac{\sqrt{2}G_F M_{H_2}^3}{32\pi} (1 - 4\kappa_Z + 12\kappa_Z^2)(1 - 4\kappa_Z)^{1/2} \delta_Z \quad (20)$$

with $\kappa_Z = M_Z^2/M_{H_2}^2$ and $\delta_Z = 1$. If $M_{H_2} > 2m_t$ then the decay channel $H_2 \rightarrow t\bar{t}$ is open:

$$\Gamma(H \rightarrow t\bar{t}) = \frac{3G_F m_t^2}{4\sqrt{2}\pi} M_H \beta_t^3 \quad (21)$$

where $\beta_t = (1 - 4m_t^2/M_{H_2}^2)^{1/2}$. All other decays of H_2 to SM particles (e.g. $H_2 \rightarrow b\bar{b}, \tau^+\tau^-$) have negligibly small partial widths for $M_{H_2} > 200$ GeV. Note that other decay channels such as $H_2 \rightarrow H^\pm W$, $H_2 \rightarrow H_1 W$ and $H_2 \rightarrow A^0 Z$ are suppressed by the small mixing between the doublet and triplet fields, and so can be neglected.

V. NUMERICAL ANALYSIS

We now study the magnitude of the branching ratios of the decays channels $H_2 \rightarrow \phi\phi$ for $\phi = H^{\pm\pm}, H^\pm, H_1, A^0$. The four important parameters are $M_{H^{\pm\pm}}, M_{H_2}, \lambda_1$ and λ_4 . The other parameters in the scalar potential are fixed as $\lambda_2 = \lambda_3 = 0.5$ and $v_\Delta = 10^{-2}$ MeV, the latter choice ensuring that the decays $H^{\pm\pm} \rightarrow \ell^\pm \ell^\pm$ are dominant. These latter three parameters appear in the expressions for the masses of the triplet scalars in eq. (9) to eq. (12) but their effect is essentially negligible, even for the case of $v_\Delta = 1$ GeV. We will present results for $M_{H^{\pm\pm}} = 90$ GeV, 150 GeV, 200 GeV and 300 GeV. As explained in the previous section, the choice of $M_{H^{\pm\pm}} = 90$ GeV requires small BRs ($< 3\%$) for the decay channels $H^{\pm\pm} \rightarrow e^\pm e^\pm, e^\pm \mu^\pm$ and $\mu^\pm \mu^\pm$ (and consequently large BRs to channels involving τ) in order to respect the limits from the direct searches for $H^{\pm\pm}$. Larger values ($\gg 3\%$) of $\text{BR}(H^{\pm\pm} \rightarrow e^\pm e^\pm, e^\pm \mu^\pm, \mu^\pm \mu^\pm)$ are permitted as $M_{H^{\pm\pm}}$ increases.

Fig. (1a) shows the branching ratios of H_2 as a function of M_{H_2} . We take $M_{H^{\pm\pm}} = 90$ GeV, $\lambda = 1$, and $\lambda_4 = 0.8$ (the latter choice gives $M_{H^\pm} = 142$ GeV and $M_{A^0, H^0} = 179$ GeV). The magnitude of $\text{BR}(H_2 \rightarrow H^{++}H^{--})$ can reach 65% for $M_{H_2} = 200$ GeV, and stays as the dominant channel until $M_{H_2} \sim 260$ GeV, at which $H_2 \rightarrow WW$ becomes dominant. $\text{BR}(H_2 \rightarrow H^{++}H^{--})$ falls below $\text{BR}(H_2 \rightarrow ZZ)$ at around $M_{H_2} = 320$ GeV. This dependence on M_{H_2} can be explained by the fact that the partial widths of $H_2 \rightarrow WW, ZZ$ are proportional to $M_{H_2}^3$, and so ultimately these channels will dominate for larger M_{H_2} . The other decays of H_2 to two triplet scalars also can have sizeable branching ratios, with $\text{BR}(H_2 \rightarrow H^+H^-)$ reaching 20% at most, and exceeds $\text{BR}(H_2 \rightarrow H^{++}H^{--})$ for $M_{H_2} \gtrsim 315$ GeV. The branching ratios of $H_2 \rightarrow A^0 A^0$ and $H_2 \rightarrow H_1 H_1$ are equal; they are plotted individually and their sum peaks at $\sim 10\%$. In fig. (1b) we show contours of $\text{BR}(H_2 \rightarrow H^{++}H^{--})$ in the plane $[M_{H_2}, \lambda_1]$.

As expected, $\text{BR}(H_2 \rightarrow H^{++}H^{--})$ takes its largest values for large λ_1 and light M_{H_2} , with $\text{BR}(H_2 \rightarrow H^{++}H^{--}) > 90\%$ being possible. We note that such a scenario would render the searches for $H_2 \rightarrow WW, ZZ$ ineffective until a very large amount of integrated luminosity is obtained. In fig. (1c) we show contours of $\text{BR}(H_2 \rightarrow H^{++}H^{--})$ in the plane $[\lambda_4, \lambda_1]$, fixing $M_{H_2} = 300$ GeV. For $\lambda_4 \gtrsim 1$ only the decay $H_2 \rightarrow H^{++}H^{--}$ is open kinematically and so the contours are horizontal. For $\lambda_4 = 0$ all the triplet scalars are degenerate and thus all four decay channels are open. Figs. 2,3 and 4 are analogies of fig. 1, but with $M_{H^{\pm\pm}} = 150$ GeV, 200 GeV and 300 GeV respectively. In all figures we take $M_{H_2} > 2M_{H^{\pm\pm}}$. One can see similar qualitative behaviour, but since the lowest value of M_{H_2} is larger in figs. 2,3 and 4 than in fig. 1, the maximum values of $\text{BR}(H_2 \rightarrow H^{++}H^{--})$ are less than in fig.1. However, in fig. 2b, fig. 3b and fig. 4b it can be seen that $\text{BR}(H_2 \rightarrow H^{++}H^{--}) > 50\%, 25\%, 5\%$ respectively is possible for $\lambda_1 \gtrsim 3$.

It clear that $\text{BR}(H_2 \rightarrow H^{++}H^{--})$ can be sizeable, and we will now quantify the magnitude of the pair production of $H^{\pm\pm}$ which originates from production and decay of H_2 . At hadron colliders H_2 is dominantly created via gluon-gluon fusion, $gg \rightarrow H_2$. For $M_{H_2} = 2M_{H^{\pm\pm}}$ the cross section of $gg \rightarrow H_2$ at the LHC is significantly larger than the cross section for the direct production mechanisms of $H^{\pm\pm}$ (i.e. $q\bar{q} \rightarrow \gamma^*, Z^* \rightarrow H^{++}H^{--}$ and $q'\bar{q} \rightarrow W \rightarrow H^{\pm\pm}H^\mp$). However, the same is not true at the Tevatron, and $\sigma(gg \rightarrow H_2) \lesssim \sigma(q\bar{q} \rightarrow \gamma^*, Z^* \rightarrow H^{++}H^{--})$ for $M_{H_2} > 2M_{H^{\pm\pm}}$.

We introduce the ratio R , defined by:

$$R = \frac{\sigma(gg \rightarrow H_2) \times \text{BR}(H_2 \rightarrow H^{++}H^{--})}{\sigma(q\bar{q} \rightarrow \gamma^*, Z^* \rightarrow H^{++}H^{--})} \quad (22)$$

The denominator in eq. (22) is the conventional mechanism for production of $H^{++}H^{--}$, which is assumed in the ongoing searches for $H^{\pm\pm}$. The numerator is a novel mechanism which contributes when $\text{BR}(H_2 \rightarrow H^{++}H^{--}) \neq 0$. We will now study the magnitude of the ratio R at the LHC (with $\sqrt{s} = 7$ TeV and 14 TeV) and at the Tevatron. In Fig. 5 we plot R as a function of M_{H_2} at the LHC with $\sqrt{s} = 14$ TeV, for $M_{H^{\pm\pm}} = 90$ GeV, 150 GeV, 200 GeV and 300 GeV. The factorisation scale and normalisation scale are both taken to be M_{H_2} for $gg \rightarrow H_2$, while for $q\bar{q} \rightarrow \gamma^*, Z^* \rightarrow H^{++}H^{--}$ both scales are taken to be the partonic centre-of-mass energy. We use CTEQ6L1 parton distribution functions [45] with the leading-order partonic cross section for $gg \rightarrow H_2$ [46]. We do not apply QCD K factors which, would increase the value of R because the ratio of the K factors for $\sigma(gg \rightarrow H_2)$ [47] and $\sigma(q\bar{q} \rightarrow \gamma^*, Z^* \rightarrow H^{++}H^{--})$ [10] is about 1.4 in the region of interest of M_{H_2} and $M_{H^{\pm\pm}}$.

In fig. (5a) we take $M_{H^{\pm\pm}} = 90$ GeV, which fixes the value of $\sigma(q\bar{q} \rightarrow H^{++}H^{--})$, and $\lambda_4 = 0.8$. We take $\lambda_1 = 1$ and 4. If $\lambda_1 = 1$ one can see that $R = 4.7$ for $M_{H_2} = 200$ GeV, and $R > 1$ for $M_{H_2} < 290$ GeV. If $\lambda_1 = 4$, one finds that $R = 7.0$ for $M_{H_2} = 200$ GeV, and $R > 1$ for $M_{H_2} < 420$ GeV. The noticeable drop in the value of R for $M_{H_2} \sim 280$ GeV is due to the opening of the decay channel $H_2 \rightarrow H^+H^-$ (see fig. (1a)). Both $\sigma(gg \rightarrow H_2)$ and $\text{BR}(H_2 \rightarrow H^{++}H^{--})$ are decreasing functions of M_{H_2} , which explains the overall dependence of R on M_{H_2} . Note that R does not fall so sharply with M_{H_2} in the region $320 \text{ GeV} < M_{H_2} < 380$ GeV, because $\sigma(gg \rightarrow H_2)$ increases in magnitude up to a local maximum at $M_{H_2} = 2m_t$, before decreasing again. In fig. (5b) we take $M_{H^{\pm\pm}} = 150$ GeV, and $R \sim 16$ for $M_{H_2} = 2m_t$ and $\lambda_1 = 4$. Larger values of R are attainable because the magnitude of $\sigma(q\bar{q} \rightarrow \gamma^*, Z^* \rightarrow H^{++}H^{--})$ (i.e. the denominator eq. (22)) diminishes considerably when going from $M_{H^{\pm\pm}} = 90$ GeV to $M_{H^{\pm\pm}} = 150$ GeV, while the corresponding decrease

in $\sigma(gg \rightarrow H_2)$ for larger M_{H_2} is relatively less. In fig. (5c) (for $M_{H^{\pm\pm}} = 200$ GeV) the maximum value is $R \sim 19$, and in fig. (5d) the maximum value is $R \sim 4$. It is evident that there is a sizeable parameter space for $R > 1$, and thus $gg \rightarrow H_2$ could give a significant (or even dominant) contribution to the pair production of $H^{\pm\pm}$ at the LHC. We also note that the decay $H_2 \rightarrow H^+H^-$ (which can have a large BR in fig. (1a) \rightarrow fig. (4a)) can lead to additional production of $H^{++}H^{--}$ because the branching ratio of the decay $H^\pm \rightarrow H^{\pm\pm}W^*$ can be large in a sizeable parameter space of $[v_\Delta, M_{H^\pm} - M_{H^{\pm\pm}}]$, as shown in [48]. In fact, in fig. (1a) \rightarrow fig. (4a) the mass splitting ($M_{H^\pm} - M_{H^{\pm\pm}}$) is between 20 GeV and 52 GeV, and with our chosen value of $v_\Delta = 10^{-2}$ MeV one would have $\text{BR}(H^\pm \rightarrow H^{\pm\pm}W^*) > 99\%$.

In fig. (6) we plot the analogies of fig. (5) for the LHC with $\sqrt{s} = 7$ TeV. One sees a similar qualitative behaviour, with lower maximum values of R . In fig. (7) we plot the corresponding results for the Tevatron, for $M_{H^{\pm\pm}} = 90$ GeV and $M_{H^{\pm\pm}} = 150$ GeV. Since $\sigma(gg \rightarrow H_2) \lesssim \sigma(q\bar{q} \rightarrow \gamma^*, Z^* \rightarrow H^{++}H^{--})$ for $M_{H_2} > 2M_{H^{\pm\pm}}$ at the Tevatron, the maximum value of $R \sim 0.4$ (for $\lambda_1 = 4$) is much smaller than at the LHC and is comparable to the QCD K factor for $\sigma(q\bar{q} \rightarrow \gamma^*, Z^* \rightarrow H^{++}H^{--})$ [10].

Finally, we quantify the number of $H^{++}H^{--}$ events for a given integrated luminosity \mathcal{L} at the LHC. We introduce the parameter $N_{H^{\pm\pm}}$, which is defined as follows:

$$N_{H^{\pm\pm}} = \epsilon \times \mathcal{L} \times [\sigma(q\bar{q} \rightarrow \gamma^*, Z^* \rightarrow H^{++}H^{--}) + \sigma(gg \rightarrow H_2) \times \text{BR}(H_2 \rightarrow H^{++}H^{--})] \quad (23)$$

The efficiency ϵ is the fraction of $H^{++}H^{--}$ events which remain after all acceptance/selection cuts are imposed to reduce the background from the SM. The value of ϵ depends on which decay channel $H^{\pm\pm} \rightarrow \ell_i^\pm \ell_j^\pm$ is being considered. From the LHC simulation in [28] for the decay $H^{\pm\pm} \rightarrow \mu^\pm \mu^\pm$ with $\sqrt{s} = 14$ TeV, one can derive an approximate value of $\epsilon_{\mu\mu} = 0.73$ for $M_{H^{\pm\pm}} = 600$ GeV and $\epsilon_{\mu\mu} = 0.64$ for $M_{H^{\pm\pm}} = 300$ GeV. As expected, the efficiency is greater for larger $M_{H^{\pm\pm}}$, since the leptons originating from $H^{\pm\pm}$ are more energetic. Extrapolating these values to the region of $M_{H^{\pm\pm}} < 300$ GeV (the mass region on which we will focus) one roughly obtains $0.5 < \epsilon_{\mu\mu} < 0.6$. The efficiencies for the decay channels $H^{\pm\pm} \rightarrow e^\pm e^\pm$ and $H^{\pm\pm} \rightarrow e^\pm \mu^\pm$ are expected to be similar in magnitude to $\epsilon_{\mu\mu}$ (see [30]). The efficiencies for the decays of $H^{\pm\pm}$ to final states involving a τ lepton are much lower e.g. in [30] one can derive $\epsilon_{\mu\tau} \sim 0.02$ for the channel $H^{\pm\pm} \rightarrow \mu^\pm \tau^\pm$, with even lower values for the channel $H^{\pm\pm} \rightarrow \tau^\pm \tau^\pm$. We will show results for the decay mode $H^{\pm\pm} \rightarrow \mu^\pm \mu^\pm$, for $M_{H^{\pm\pm}} = 90$ GeV, 150 GeV, 200 GeV and 300 GeV. The strongest lower bounds on $M_{H^{\pm\pm}}$ in this channel (assuming a branching ratio of 100%) are $M_{H^{\pm\pm}} > 156$ GeV from the LHC in [30] and $M_{H^{\pm\pm}} > 245$ GeV from the Tevatron in [44], both limits being preliminary results. For the case of $\text{BR}(H^{\pm\pm} \rightarrow \mu^\pm \mu^\pm) < 100\%$, one can derive from [44] the approximate limits $M_{H^{\pm\pm}} \gtrsim 100$ GeV, $\gtrsim 150$ GeV and $\gtrsim 200$ GeV for $\text{BR} \gtrsim 3\%$, $\gtrsim 15\%$ and $\gtrsim 40\%$, respectively. We do not include these values of $\text{BR}(H^{\pm\pm} \rightarrow \mu^\pm \mu^\pm)$ when showing results for $N_{H^{\pm\pm}}$. In future searches which require three or four leptons (as done in the LHC search in [30]) the event number $N_{H^{\pm\pm}}$ in eq. (23) needs to be scaled by a multiplicative factor of $[\text{BR}(H^{\pm\pm} \rightarrow \ell_i^\pm \ell_j^\pm)]^2$. As explained above, this factor is necessarily less than unity if one considers $M_{H^{\pm\pm}} < 245$ GeV with decay $H^{\pm\pm} \rightarrow \mu^\pm \mu^\pm$.

In fig. (8) we show $N_{H^{\pm\pm}}$ in the plane $[M_{H_2}, \lambda_1]$ for $\sqrt{s} = 14$ TeV with $\mathcal{L} = 30 \text{ fb}^{-1}$. We use $\epsilon_{\mu\mu} = 0.64$ for $M_{H^{\pm\pm}} = 300$ GeV, and $\epsilon_{\mu\mu} = 0.50$ for the other chosen values of $M_{H^{\pm\pm}}$ (90 GeV, 150 GeV, 200 GeV). The contribution to $N_{H^{\pm\pm}}$ from $q\bar{q} \rightarrow \gamma^*, Z^* \rightarrow H^{++}H^{--}$ alone does not depend on M_{H_2} and λ_1 , and is roughly equal to 20500, 3270, 1130 and 280 for $M_{H^{\pm\pm}} = 90$ GeV, 150 GeV, 200 GeV and 300 GeV respectively. In each panel in fig. (8) the contour with the lowest number of events corresponds to a value of $N_{H^{\pm\pm}}$ which is slightly

larger than the above values for $N_{H^{\pm\pm}}$ from $q\bar{q} \rightarrow \gamma^*, Z^* \rightarrow H^{++}H^{--}$ alone. We emphasise that the displayed $N_{H^{\pm\pm}}$ for $M_{H^{\pm\pm}} = 90$ GeV, 150 GeV and 200 GeV need to be multiplied by the square of BR (for a future three or four lepton search) where $\text{BR} \lesssim 3\%$, $\lesssim 15\%$ and $\lesssim 40\%$ in order to comply with the mass limits in [44]. Fig. (8) can also be applied to other decay channels such as $H^{\pm\pm} \rightarrow \mu^\pm \tau^\pm$ after multiplying $N_{H^{\pm\pm}}$ by $\epsilon_{\mu\tau}/\epsilon_{\mu\mu} \sim 1/30$. Clearly, the contribution from $\sigma(gg \rightarrow H_2) \times \text{BR}(H_2 \rightarrow H^{++}H^{--})$ could significantly enhance the number of $H^{++}H^{--}$ events at the LHC, provided that $M_{H_2} > 2M_{H^{\pm\pm}}$ and λ_1 is not very small. Since it is not expected that $M_{H_2} \gtrsim 700$ GeV (from considering constraints from perturbativity and unitarity e.g. see [33]), the enhancement from $\sigma(gg \rightarrow H_2) \times \text{BR}(H_2 \rightarrow H^{++}H^{--})$ is limited to the region $M_{H^{\pm\pm}} \lesssim 350$ GeV. However, its contribution would allow the possibility of probing smaller values of $\text{BR}(H^{\pm\pm} \rightarrow \ell_i^\pm \ell_j^\pm)$ for a given value of $M_{H^{\pm\pm}}$ (provided that $M_{H_2} > 2M_{H^{\pm\pm}}$).

In fig. (9) we show $N_{H^{\pm\pm}}$ for $\sqrt{s} = 7$ TeV with $\mathcal{L}=2 \text{ fb}^{-1}$. We take a slightly lower efficiency of $\epsilon_{\mu\mu} = 0.4$ for $M_{H^{\pm\pm}} = 90$ GeV, 150 GeV and 200 GeV, which is in rough agreement with the value for the channel $H^{\pm\pm} \rightarrow \mu^\pm \mu^\pm$ in the experimental search at $\sqrt{s} = 7$ TeV in [30]. For $M_{H^{\pm\pm}} = 300$ GeV we take $\epsilon_{\mu\mu} = 0.5$. Again, the enhancement from $\sigma(gg \rightarrow H_2) \times \text{BR}(H_2 \rightarrow H^{++}H^{--})$ can be sizeable, and could lead to a quicker discovery of a light $H^{\pm\pm}$ with $\text{BR}(H^{\pm\pm} \rightarrow \ell_i^\pm \ell_j^\pm) < 100\%$. We do not plot an analogous figure for the Tevatron since the maximum value of R is much smaller than at the LHC, as shown in fig. (6).

Finally, we emphasise that the parameter space of $M_{H_2} > 2M_{H^{\pm\pm}}$ will be probed by two distinct searches with the LHC data taken at $\sqrt{s} = 7$ TeV: i) the search for $H_2 \rightarrow WW, ZZ$ (with first results in [34, 35]), and ii) the search for $q\bar{q} \rightarrow \gamma^*, Z^* \rightarrow H^{++}H^{--}$ (with first results in [30], and a simulation in [49]). The run at $\sqrt{s} = 7$ TeV, with possibly up to 5 fb^{-1} of integrated luminosity, has the potential to exclude or provide evidence for a SM-like Higgs boson with $200 \text{ GeV} < M_{H_2} < 500 \text{ GeV}$ at a high confidence level. Therefore the scenario of $M_{H_2} > 2M_{H^{\pm\pm}}$ and its possible impact on the direct searches for $H^{\pm\pm}$ should be clarified within the next two years.

VI. CONCLUSIONS

Doubly charged Higgs bosons ($H^{\pm\pm}$), which arise in the Higgs Triplet Model (HTM) of neutrino mass generation, are being searched for at the Tevatron and at the LHC. The ongoing searches assume the production mechanisms $q\bar{q} \rightarrow \gamma^*, Z^* \rightarrow H^{++}H^{--}$ and $q'\bar{q} \rightarrow W^* \rightarrow H^{\pm\pm}H^\mp$, with the leptonic decay $H^{\pm\pm} \rightarrow \ell_i^\pm \ell_j^\pm$. We proposed an additional production mechanism for $H^{\pm\pm}$, which becomes possible if the SM-like Higgs boson in the HTM (H_2) is heavy enough to decay to a pair of on-shell $H^{\pm\pm}$. We quantified the magnitude of the branching ratio of $H_2 \rightarrow H^{++}H^{--}$, and showed that it can be large ($\gg 10\%$) if a quartic coupling in the scalar potential is sizeable, $\lambda_1 > 1$. We performed a numerical study of the production rate for H_2 via gluon-gluon fusion, $gg \rightarrow H_2$, followed by the decay $H_2 \rightarrow H^{++}H^{--}$, and we showed that its cross section at the LHC can be greater than that of $q\bar{q} \rightarrow \gamma^*, Z^* \rightarrow H^{++}H^{--}$ in a sizeable parameter space of $[\lambda_1, M_{H_2}]$ (with $M_{H_2} > 2M_{H^{\pm\pm}}$). In the optimal case (e.g. $\lambda_1 = 4$, $M_{H_2} \sim 420$ GeV and $M_{H^{\pm\pm}} = 200$ GeV) the ratio of cross sections can be as large as nineteen. We note that our analysis was carried out using the leading-order cross sections only, and the inclusion of QCD K factors would provide a further enhancement of 40% in the above ratio. Such an additional source of $H^{++}H^{--}$ would enable smaller values of the branching ratio of $H^{\pm\pm} \rightarrow \ell_i^\pm \ell_j^\pm$ to be probed at the LHC.

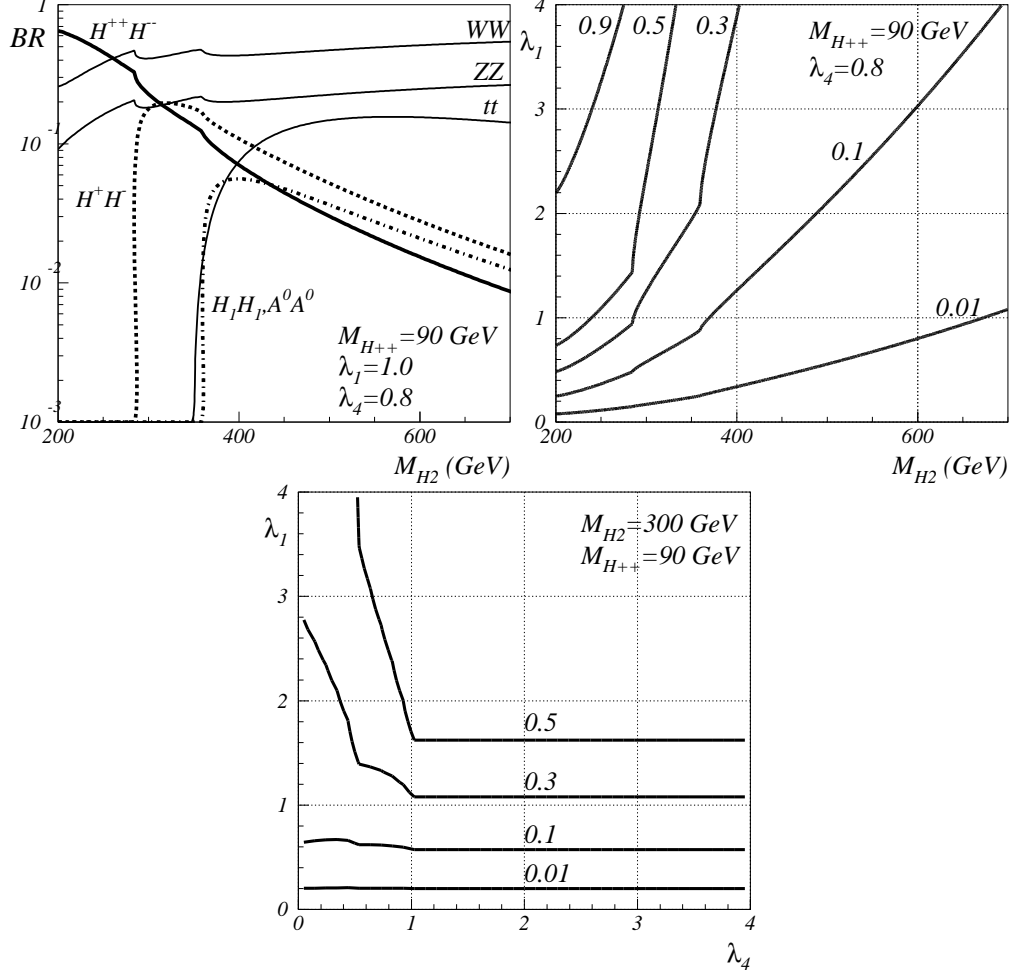


FIG. 1: Upper left panel a): branching ratios of H_2 as a function of M_{H_2} . Upper right panel b): Contours of $\text{BR}(H_2 \rightarrow H^{++}H^{--})$ in the plane $[M_{H_2}, \lambda_1]$. Lower panel c): Contours of $\text{BR}(H_2 \rightarrow H^{++}H^{--})$ in the plane $[\lambda_4, \lambda_1]$. In all figures $M_{H^{\pm\pm}} = 90$ GeV. In a) and b) $\lambda_4 = 0.8$, which gives $M_{H^\pm} = 142$ GeV and $M_{A^0, H_1} = 179$ GeV. In c) $M_{H_2} = 300$ GeV.

The case of $M_{H_2} > 2M_{H^{\pm\pm}}$ necessarily requires $M_{H_2} \gtrsim 200$ GeV, and this mass region is now being probed for the first time at the LHC for the decay channels of H_2 to SM particles, $H_2 \rightarrow WW$ and $H_2 \rightarrow ZZ$. The possibility of a SM-like Higgs boson in the HTM with $M_{H_2} > 2M_{H^{\pm\pm}}$ and its potential impact on the direct searches for $H^{\pm\pm}$ should be clarified within the $\sqrt{s} = 7$ TeV run at the LHC.

Acknowledgements

We thank Hiroaki Sugiyama and Abdesslam Arhrib for useful discussions. A.G.A was supported by a Marie Curie Incoming International Fellowship, FP7-PEOPLE-2009-IIF, Contract No. 252263. This work is supported in part by the NExT Institute.

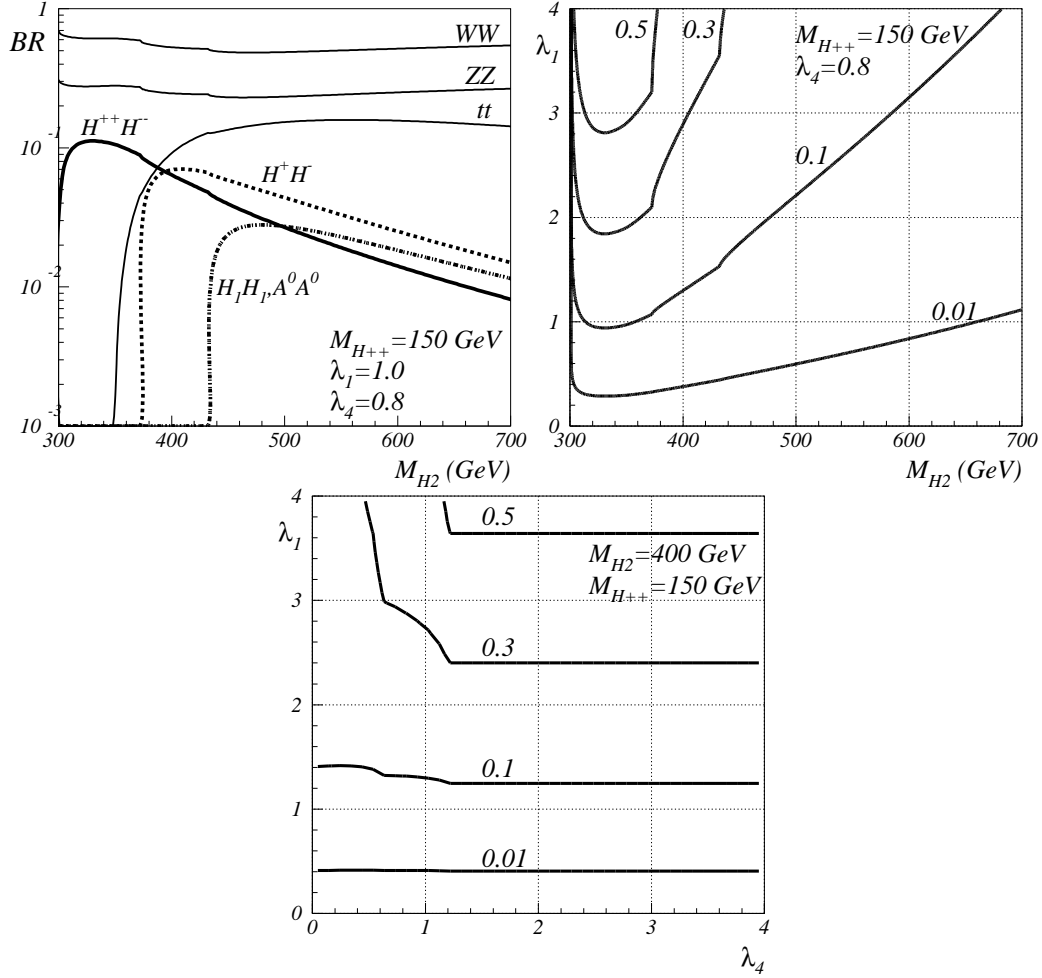


FIG. 2: Upper left panel a): branching ratios of H_2 as a function of M_{H_2} . Upper right panel b): Contours of $\text{BR}(H_2 \rightarrow H^{++}H^{--})$ in the plane $[M_{H_2}, \lambda_1]$. Lower panel c): Contours of $\text{BR}(H_2 \rightarrow H^{++}H^{--})$ in the plane $[\lambda_4, \lambda_1]$. In all figures $M_{H^{\pm\pm}} = 150$ GeV. In a) and b) $\lambda_4 = 0.8$, which gives $M_{H^\pm} = 186$ GeV and $M_{A^0, H_1} = 216$ GeV. In c) $M_{H_2} = 400$ GeV.

Note Added

After submission of this paper, the LHC searches for the SM Higgs boson were updated with $\mathcal{L} = 1.1 \text{ fb}^{-1}$ [50]. For the region $M_{H_2} > 200$ GeV, both of the CMS and ATLAS collaborations use the decay channel $H_2 \rightarrow ZZ$, with subsequent decays $ZZ \rightarrow \ell^+\ell^-\nu\nu$, $ZZ \rightarrow \ell^+\ell^-q\bar{q}$ and $ZZ \rightarrow \ell^+\ell^-\ell^+\ell^-$. CMS also search for $H_2 \rightarrow WW$ with the decay mode $WW \rightarrow \ell\nu\ell\nu$, while ATLAS search for $H_2 \rightarrow WW$ with the decay mode $WW \rightarrow \ell\nu q'\bar{q}$. After combining the results from these four distinct channels, both collaborations exclude at 95% c.l the mass range $295 \text{ GeV} < M_{H_2} < 450 \text{ GeV}$. This does not preclude a sizeable value of R in the HTM, e.g. from fig. 6c, one can see that $7 > R > 1$ in the interval $450 \text{ GeV} < M_{H_2} < 600 \text{ GeV}$, for $\lambda_1 = 4$ and $\sqrt{s} = 7$ TeV (and not including the

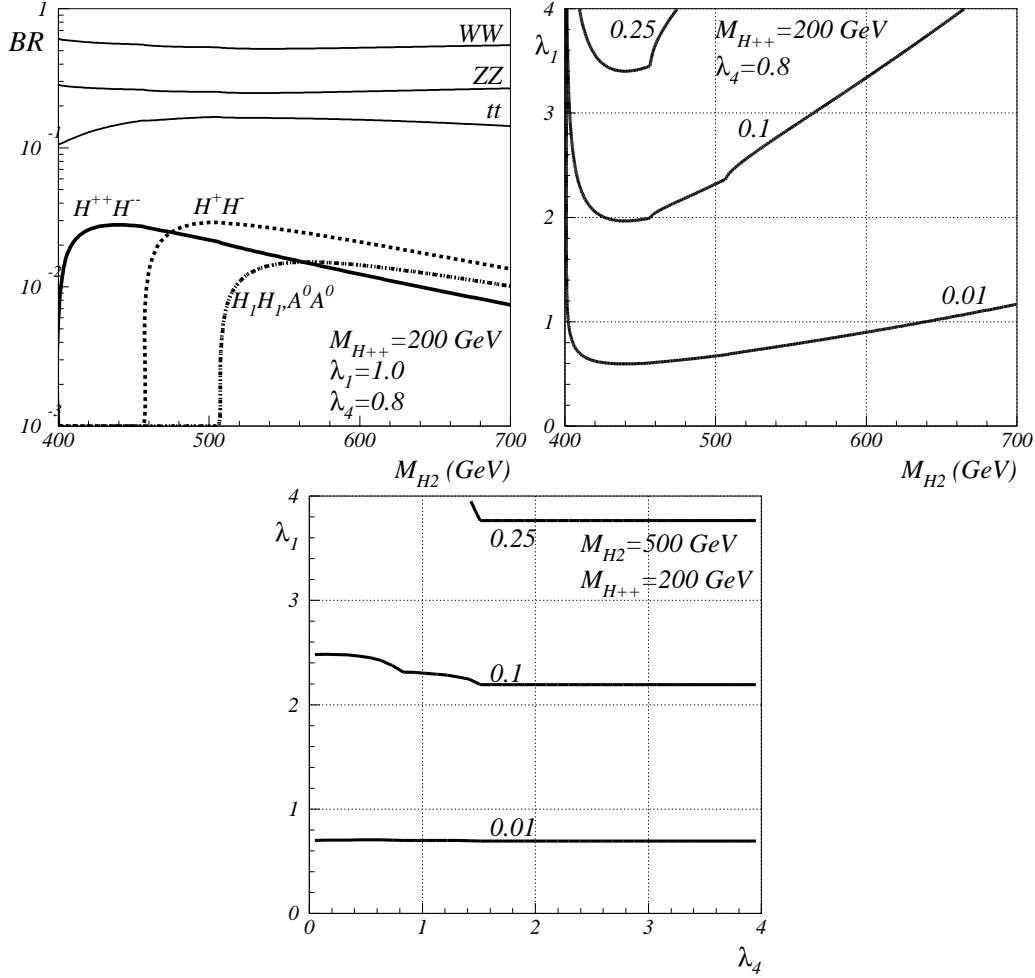


FIG. 3: Upper left panel a): branching ratios of H_2 as a function of M_{H_2} . Upper right panel b): Contours of $\text{BR}(H_2 \rightarrow H^{++}H^{--})$ in the plane $[M_{H_2}, \lambda_1]$. Lower panel c): Contours of $\text{BR}(H_2 \rightarrow H^{++}H^{--})$ in the plane $[\lambda_4, \lambda_1]$. In all figures $M_{H^{\pm\pm}} = 200$ GeV. In a) and b) $\lambda_4 = 0.8$, which gives $M_{H^\pm} = 228$ GeV and $M_{A^0, H_1} = 253$ GeV. In c) $M_{H_2} = 500$ GeV.

enhancement from the QCD K factor).

-
- [1] Y. Fukuda *et al.* [Super-Kamiokande Collaboration], Phys. Rev. Lett. **81**, 1562 (1998).
 - [2] Y. Kuno and Y. Okada, Rev. Mod. Phys. **73**, 151 (2001); M. Raidal *et al.*, Eur. Phys. J. C **57**, 13 (2008).
 - [3] W. Konetschny and W. Kummer, Phys. Lett. B **70**, 433 (1977).
 - [4] R. N. Mohapatra and G. Senjanovic, Phys. Rev. Lett. **44**, 912 (1980).
 - [5] M. Magg and C. Wetterich, Phys. Lett. B **94**, 61 (1980); G. Lazarides, Q. Shafi and C. Wetterich, Nucl. Phys. B **181**, 287 (1981).
 - [6] J. Schechter and J. W. F. Valle, Phys. Rev. D **22**, 2227 (1980).
 - [7] T. P. Cheng and L. F. Li, Phys. Rev. D **22**, 2860 (1980).

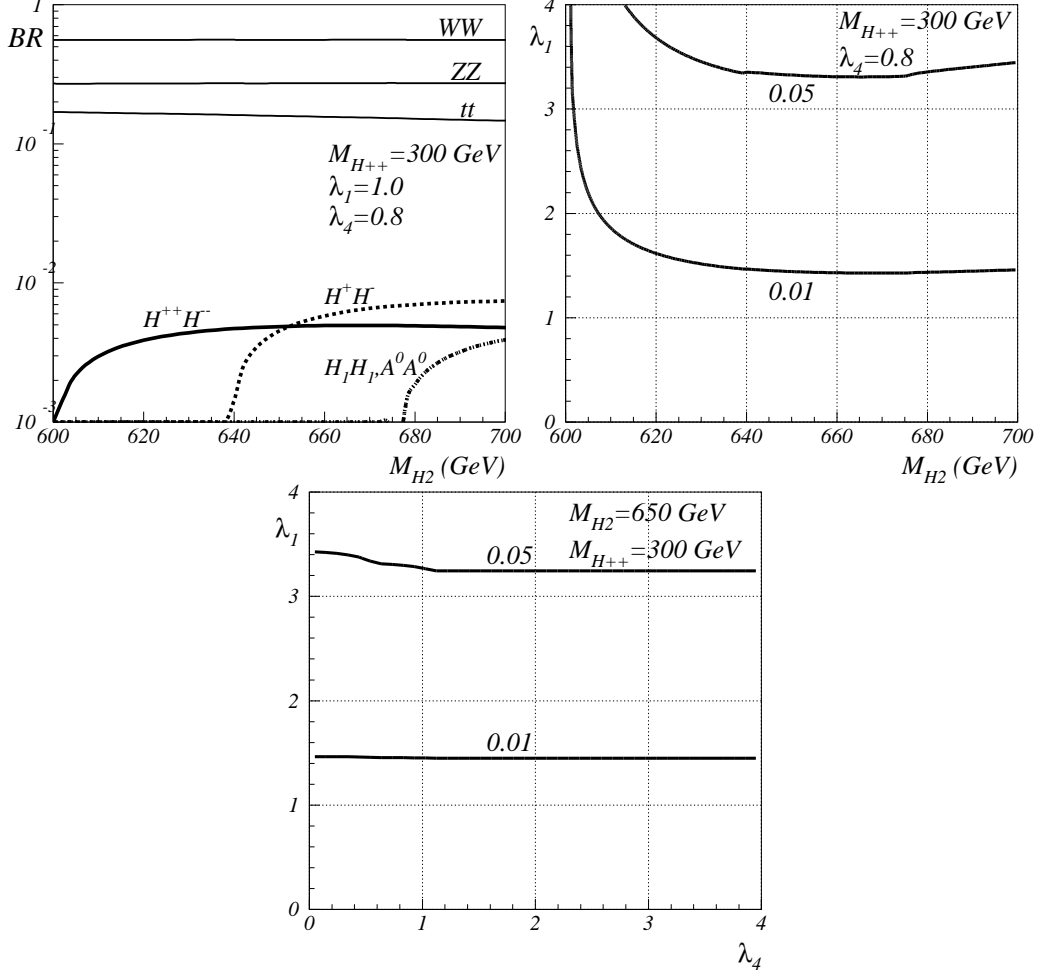


FIG. 4: Upper left panel a): branching ratios of H_2 as a function of M_{H_2} . Upper right panel b): Contours of $\text{BR}(H_2 \rightarrow H^{++}H^{--})$ in the plane $[M_{H_2}, \lambda_1]$. Lower panel c): Contours of $\text{BR}(H_2 \rightarrow H^{++}H^{--})$ in the plane $[\lambda_4, \lambda_1]$. In all figures $M_{H^{\pm\pm}} = 300$ GeV. In a) and b) $\lambda_4 = 0.8$, which gives $M_{H^\pm} = 320$ GeV and $M_{A^0, H_1} = 338$ GeV. In c) $M_{H_2} = 650$ GeV.

- [8] V. D. Barger, H. Baer, W. Y. Keung and R. J. N. Phillips, Phys. Rev. D **26**, 218 (1982).
- [9] J. F. Gunion, J. Grifols, A. Mendez, B. Kayser and F. I. Olness, Phys. Rev. D **40**, 1546 (1989); J. F. Gunion, C. Loomis and K. T. Pitts, eConf **C960625**, LTH096 (1996) [arXiv:hep-ph/9610237].
- [10] M. Muhlleitner and M. Spira, Phys. Rev. D **68**, 117701 (2003).
- [11] T. Han, B. Mukhopadhyaya, Z. Si and K. Wang, Phys. Rev. D **76**, 075013 (2007).
- [12] K. Huitu, J. Maalampi, A. Pietila and M. Raidal, Nucl. Phys. B **487**, 27 (1997).
- [13] B. Dion, T. Gregoire, D. London, L. Marleau and H. Nadeau, Phys. Rev. D **59**, 075006 (1999).
- [14] A. G. Akeroyd and M. Aoki, Phys. Rev. D **72**, 035011 (2005).
- [15] D. E. Acosta *et al.* [CDF Collaboration], Phys. Rev. Lett. **93**, 221802 (2004).
- [16] V. M. Abazov *et al.* [D0 Collaboration], Phys. Rev. Lett. **93**, 141801 (2004).
- [17] V. M. Abazov *et al.* [D0 Collaboration], Phys. Rev. Lett. **101**, 071803 (2008).
- [18] T. Aaltonen *et al.* [The CDF Collaboration], Phys. Rev. Lett. **101**, 121801 (2008).

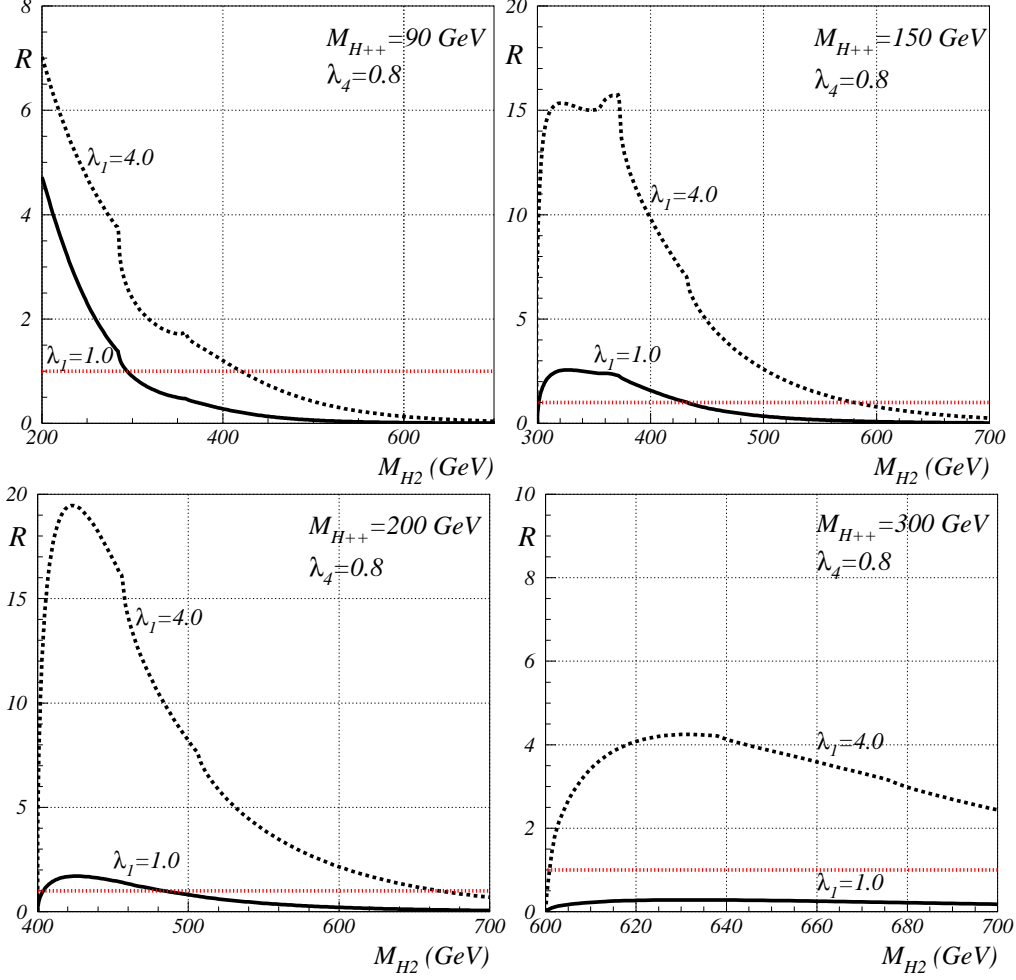


FIG. 5: The ratio $R = \sigma(gg \rightarrow H_2) \times \text{BR}(H_2 \rightarrow H^{++}H^{--}) / \sigma(q\bar{q} \rightarrow H^{++}H^{--})$ at the LHC (with $\sqrt{s} = 14$ TeV) as a function of M_{H_2} . The two curves are for $\lambda_1 = 1$ and $\lambda_1 = 4$, with $\lambda_4 = 0.8$. We take $M_{H^{++}} = 90$ GeV in panel (a), $M_{H^{++}} = 150$ GeV in panel (b), $M_{H^{++}} = 200$ GeV in panel (c), and $M_{H^{++}} = 300$ GeV in panel (d). The horizontal line shows $R = 1$.

- [19] E. Ma, M. Raidal and U. Sarkar, Phys. Rev. Lett. **85**, 3769 (2000); E. Ma, M. Raidal and U. Sarkar, Nucl. Phys. B **615**, 313 (2001).
- [20] E. J. Chun, K. Y. Lee and S. C. Park, Phys. Lett. B **566**, 142 (2003).
- [21] J. Garayoa and T. Schwetz, JHEP **0803**, 009 (2008).
- [22] A. G. Akeroyd, M. Aoki and H. Sugiyama, Phys. Rev. D **77**, 075010 (2008).
- [23] M. Kadastik, M. Raidal and L. Rebane, Phys. Rev. D **77**, 115023 (2008).
- [24] P. Fileviez Perez, T. Han, G. y. Huang, T. Li and K. Wang, Phys. Rev. D **78**, 015018 (2008).
- [25] F. del Aguila and J. A. Aguilar-Saavedra, Nucl. Phys. B **813**, 22 (2009).
- [26] A. G. Akeroyd and C. W. Chiang, Phys. Rev. D **80**, 113010 (2009).
- [27] G. Azuelos, K. Benslama and J. Ferland, J. Phys. G **32**, 73 (2006).
- [28] T. Rommelskirchen and T. Hebbeker, J. Phys. G **34**, N47 (2007).
- [29] A. G. Akeroyd, C. W. Chiang and N. Gaur, JHEP **1011**, 005 (2010).
- [30] CMS Collaboration, CMS PAS HIG-11-001 (March 2011).

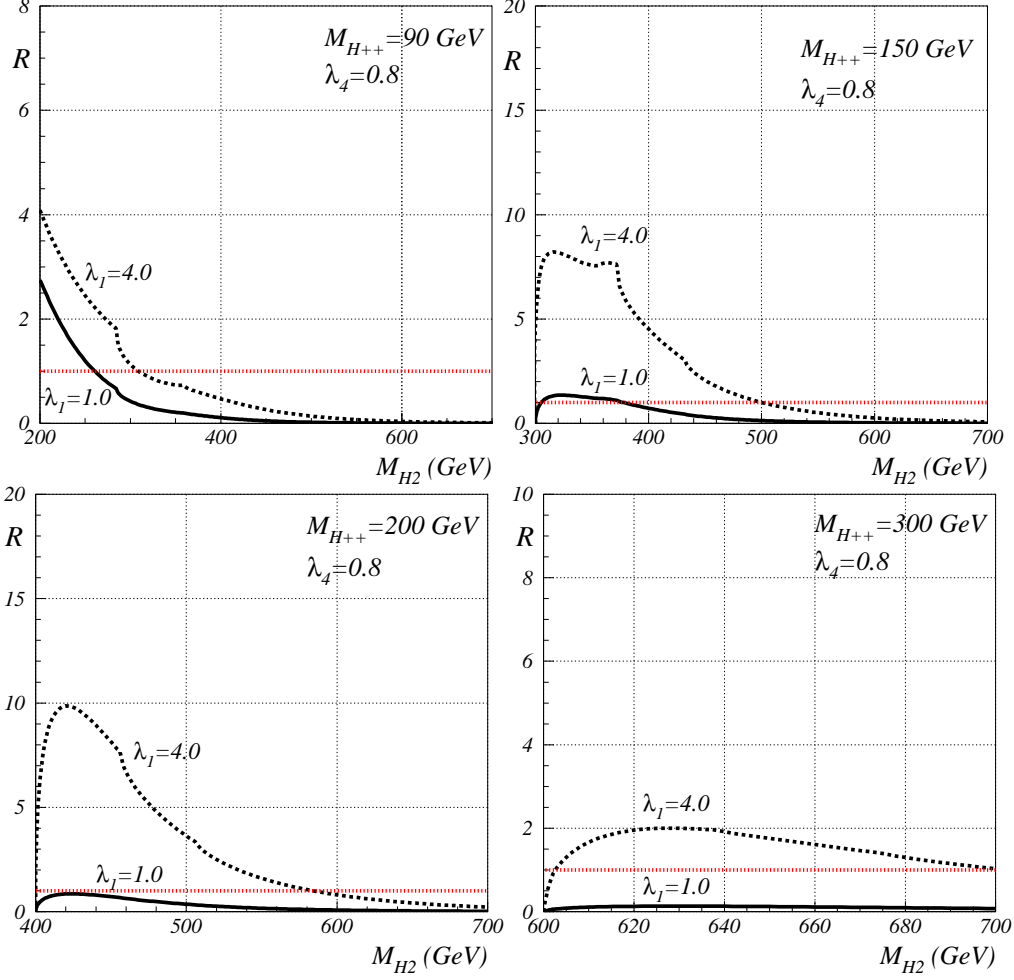


FIG. 6: The ratio $R = \sigma(gg \rightarrow H_2) \times \text{BR}(H_2 \rightarrow H^{++}H^{--}) / \sigma(q\bar{q} \rightarrow H^{++}H^{--})$ at the LHC (with $\sqrt{s} = 7$ TeV) as a function of M_{H_2} . The two curves are for $\lambda_1 = 1$ and $\lambda_1 = 4$, with $\lambda_4 = 0.8$. We take $M_{H^{\pm\pm}} = 90$ GeV in panel (a), $M_{H^{\pm\pm}} = 150$ GeV in panel (b), $M_{H^{\pm\pm}} = 200$ GeV in panel (c), and $M_{H^{\pm\pm}} = 300$ GeV in panel (d). The horizontal line shows $R = 1$.

- [31] P. Dey, A. Kundu and B. Mukhopadhyaya, J. Phys. G **36**, 025002 (2009).
- [32] A. G. Akeroyd and C. W. Chiang, Phys. Rev. D **81**, 115007 (2010).
- [33] A. Arhrib, R. Benbrik, M. Chabab, G. Moulata, M. C. Peyranere, L. Rahili and J. Ramadan, arXiv:1105.1925 [hep-ph].
- [34] ATLAS Collaboration, arXiv:1106.2748 [hep-ex].
- [35] S. Chatrchyan *et al.* [CMS Collaboration], Phys. Lett. B **699**, 25 (2011).
- [36] G. B. Gelmini and M. Roncadelli, Phys. Lett. B **99**, 411 (1981).
- [37] J. Schechter and J. W. F. Valle, Phys. Rev. D **25**, 774 (1982); M. A. Diaz, M. A. Garcia-Jareno, D. A. Restrepo and J. W. F. Valle, Nucl. Phys. B **527**, 44 (1998); A. G. Akeroyd, M. A. Diaz, M. A. Rivera, D. Romero, Phys. Rev. **D83**, 095003 (2011).
- [38] S. K. Majee and N. Sahu, Phys. Rev. D **82**, 053007 (2010).
- [39] J. F. Gunion, R. Vega and J. Wudka, Phys. Rev. D **42**, 1673 (1990); R. Vega and D. A. Dicus, Nucl. Phys. B **329**, 533 (1990); J. Maalampi and N. Romanenko, Phys. Lett. B **532**, 202

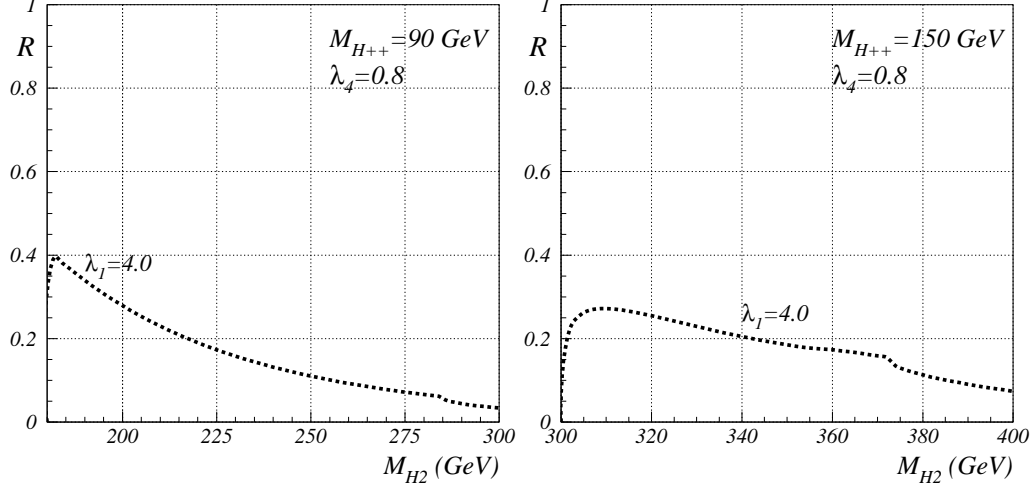


FIG. 7: The ratio $R = \sigma(gg \rightarrow H_2) \times \text{BR}(H_2 \rightarrow H^{++}H^{--}) / \sigma(q\bar{q} \rightarrow H^{++}H^{--})$ at the Tevatron (with $\sqrt{s} = 1.96$ TeV) as a function of M_{H_2} . The curves are for $\lambda_1 = 4$ and $\lambda_4 = 0.8$. We take $M_{H^{\pm\pm}} = 90$ GeV in panel (a), $M_{H^{\pm\pm}} = 150$ GeV in panel (b).

- (2002).
- [40] T. Blank and W. Hollik, Nucl. Phys. B **514**, 113 (1998); J. R. Forshaw, D. A. Ross, B. E. White, JHEP **0110**, 007 (2001); J. R. Forshaw, A. Sabio Vera, B. E. White, JHEP **0306**, 059 (2003); P. H. Chankowski, S. Pokorski and J. Wagner, Eur. Phys. J. C **50**, 919 (2007); M. C. Chen, S. Dawson and C. B. Jackson, Phys. Rev. D **78**, 093001 (2008).
 - [41] M. C. Chen, S. Dawson and T. Krupovnickas, Phys. Rev. D **74**, 035001 (2006).
 - [42] S. de Visscher, J. M. Gerard, M. Herquet, V. Lemaître and F. Maltoni, JHEP **0908**, 042 (2009).
 - [43] J. Abdallah *et al.* [DELPHI Collaboration], Phys. Lett. B **552**, 127 (2003) [arXiv:hep-ex/0303026]; G. Abbiendi *et al.* [OPAL Collaboration], Phys. Lett. B **526**, 221 (2002); P. Achard *et al.* [L3 Collaboration], Phys. Lett. B **576**, 18 (2003).
 - [44] T. Aaltonen *et al.* [CDF Collaboration], arXiv:1108.0101 [hep-ex].
 - [45] J. Pumplin, D. R. Stump, J. Huston, H. L. Lai, P. M. Nadolsky and W. K. Tung, JHEP **0207**, 012 (2002); D. Stump, J. Huston, J. Pumplin, W. K. Tung, H. L. Lai, S. Kuhlmann and J. F. Owens, JHEP **0310**, 046 (2003).
 - [46] H. M. Georgi, S. L. Glashow, M. E. Machacek and D. V. Nanopoulos, Phys. Rev. Lett. **40**, 692 (1978); M. Spira, A. Djouadi, D. Graudenz and P. M. Zerwas, Nucl. Phys. B **453**, 17 (1995).
 - [47] A. Djouadi, Phys. Rept. **457**, 1 (2008).
 - [48] A. G. Akeroyd, H. Sugiyama, [arXiv:1105.2209 [hep-ph]].
 - [49] V. Rentala, W. Shepherd, S. Su, [arXiv:1105.1379 [hep-ph]].
 - [50] Talk by W. Murray at the International Europhysics Conference on High Energy Physics, Grenoble, France, July 21-27 2011.

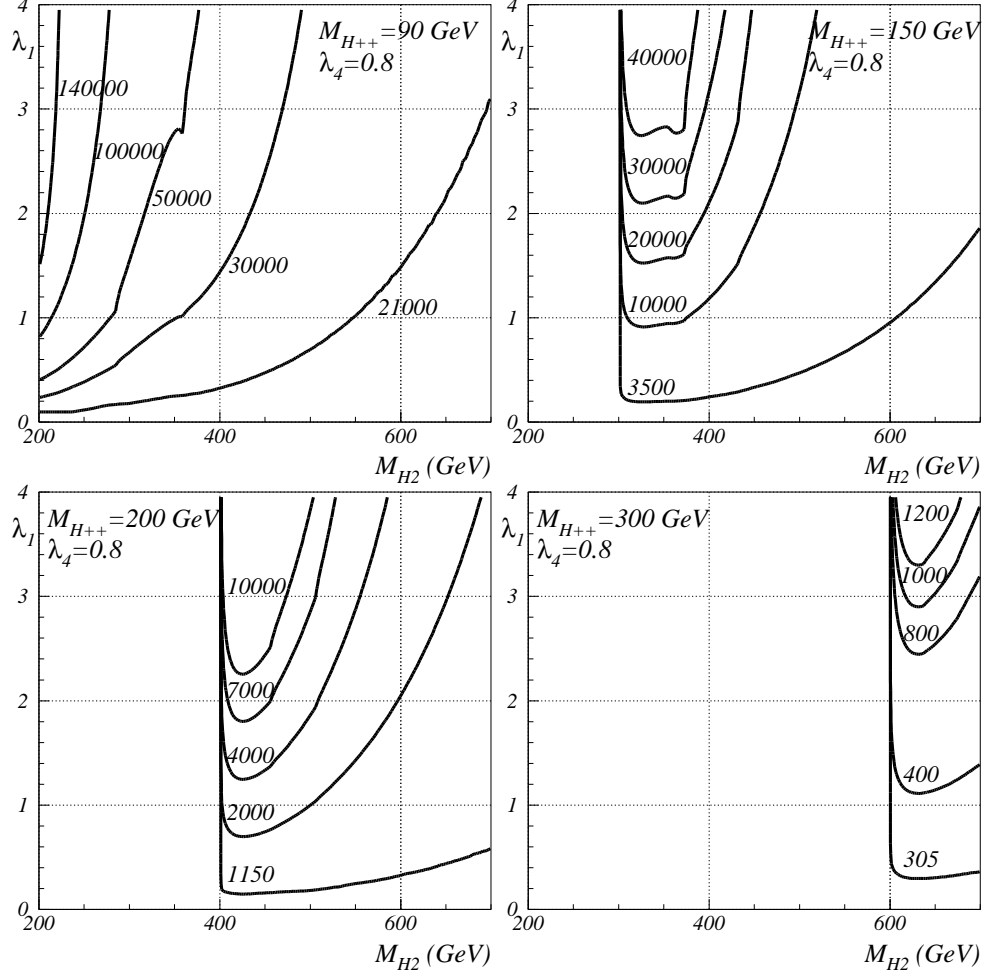


FIG. 8: The number of $H^{++}H^{--}$ events (assuming $\text{BR}(H^{\pm\pm} \rightarrow \mu^{\pm}\mu^{\pm}) = 100\%$) at the LHC with $\sqrt{s} = 14$ TeV and $\mathcal{L} = 30 \text{ fb}^{-1}$ in the plane $[M_{H_2}, \lambda_1]$. We take $M_{H^{\pm\pm}} = 90$ GeV in panel (a), $M_{H^{\pm\pm}} = 150$ GeV in panel (b), $M_{H^{\pm\pm}} = 200$ GeV in panel (c) and $M_{H^{\pm\pm}} = 300$ GeV in panel (d). In all figures $\lambda_4 = 0.8$. The number of events for $q\bar{q} \rightarrow \gamma, Z \rightarrow H^{++}H^{--}$ alone is 20500, 3270, 1130 and 299 in (a),(b),(c) and (d), respectively.

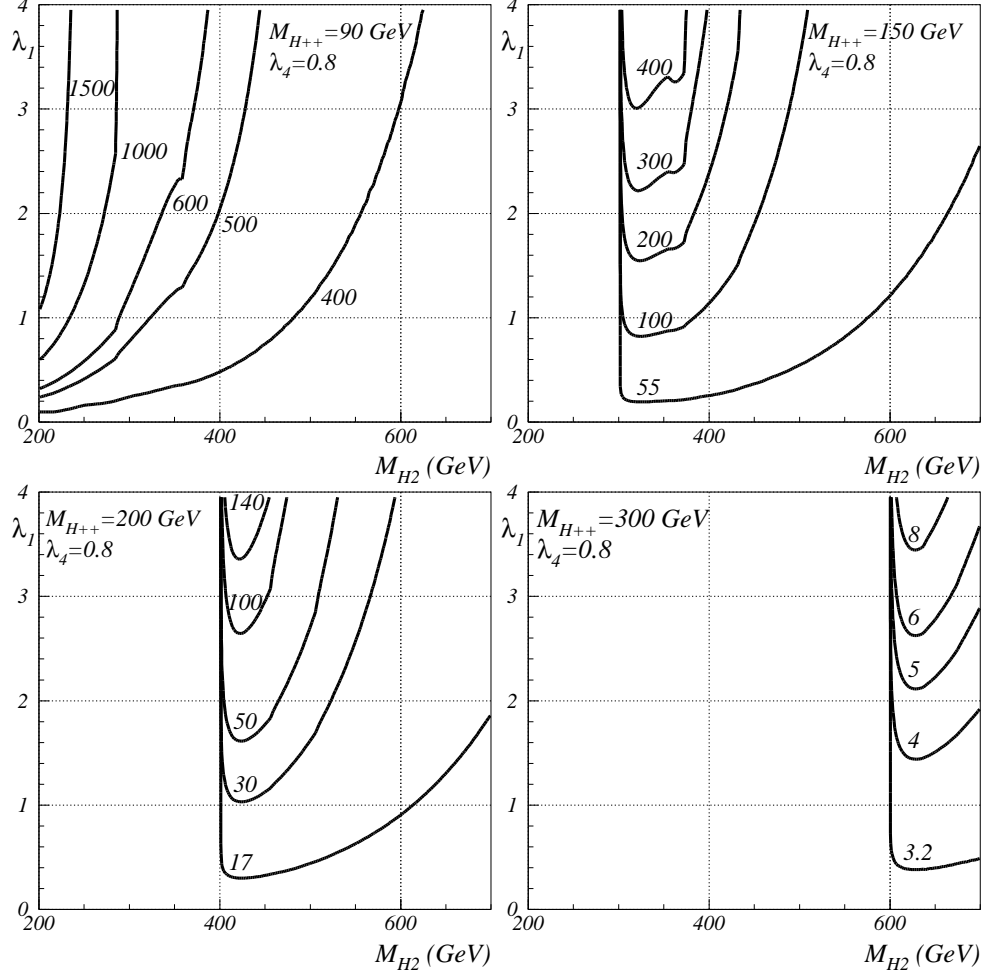


FIG. 9: The number of $H^{++}H^{--}$ events (assuming $\text{BR}(H^{\pm\pm} \rightarrow \mu^{\pm}\mu^{\pm}) = 100\%$) at the LHC with $\sqrt{s} = 7$ TeV and $\mathcal{L} = 2 \text{ fb}^{-1}$ in the plane $[M_{H_2}, \lambda_1]$. We take $M_{H^{\pm\pm}} = 90$ GeV in panel (a), $M_{H^{\pm\pm}} = 150$ GeV in panel (b), $M_{H^{\pm\pm}} = 200$ GeV in panel (c) and $M_{H^{\pm\pm}} = 300$ GeV in panel (d). In all figures $\lambda_4 = 0.8$. The number of events for $q\bar{q} \rightarrow \gamma, Z \rightarrow H^{++}H^{--}$ alone is 390, 53, 16, 3 in (a),(b),(c) and (d), respectively.